Molecular Switches

DOI: 10.1002/anie.201302587

A Directly Linked Ferrocene–Naphthalenediimide Conjugate: Precise Control of Stacking Structures of π-Systems by Redox Stimuli**

*Atsuro Takai, Takeshi Yasuda, Tomoya Ishizuka, Takahiko Kojima, and Masayuki Takeuchi**

Control and switching of the interactions between π-conjugated molecules are of great interest for the construction of functional π-assemblies toward electrical and optical nanodevices. Extensive efforts have so far been devoted to developing molecular actuators where the conformation of the related π-conjugated systems can be changed by external stimuli such as redox and light.[1] However, it remains a challenge to change the stacking structure and the electronic states of the π-conjugated molecules in a programmed manner, because covalently linked π-systems would be either too rigid or too flexible, and non-covalently linked π-systems would be too brittle to maintain their structures in solution.[2] In this context, it occurred to us that stacking conformation of the π-conjugated molecules can be regulated by associating with pivoting motion of a rigidly connected rotator.

Pivoting motion is a fundamental two-dimensional motion found not only in natural systems such as ATP synthases but also in artificial mechanical systems.[3,4] Ferrocene (Fc) has been recognized as a molecular rotational unit in which the two cyclopentadienyl (Cp) rings rotate in the horizontal direction with a small rotational barrier.[4–6] Recently, it has been reported that two π-conjugated molecules introduced on both Cp rings of Fc through covalent linkers can control the pivoting motion of Fc.[6] In these cases, however, it would be difficult to translate the pivoting motion of Fc into the stacking/destacking geometries of π-conjugated molecules, because the dynamic orientation of π-systems is equivocal. We envision that if redox-responsive π-conjugated molecules are connected directly to the molecular rotator (Fc), the dynamic orientation of the π-systems can be controlled precisely in concert with the pivoting motion of Fc. Accordingly, such a rotor-π-conjugated molecule would become an organic actuating unit for constructing new polymeric system, which deliberately undergoes contraction and expansion in length by redox stimuli.

We report herein the synthesis and the electron-transfer properties of a ferrocene derivative having two directly connected naphthalenediimide moieties (**1**; Scheme 1). We

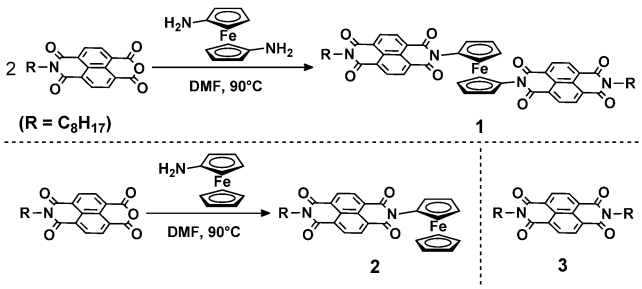

Scheme 1. Syntheses and structures of **1**, **2**, and **3**.

obtained **1** from *N*-octyl-1,4,5,8-naphthalenetetracarboxylic monoanhydride[7] and diaminoferrocene.[8] This method is an effective alternative to the conventional method to synthesize *N*-ferrocenyl naphthalimides using the corresponding naphthalimide and bromoferrocene in the presence of Cu_2O under severe conditions.[9] A corresponding 1:1 composite (**2**) and *N*,*N*′-dioctylnaphthalenediimide (**3**) were also prepared for comparison. All of the compounds were characterized by NMR, MALDI/TOF-MS, and elemental analysis (for details, see the Experimental Section and the Supporting Information, Figures S1–S4). Naphthalenediimide (NDI) was employed as a π-conjugated compound, because it is a robust π-plane acting as an electron acceptor, in contrast to Fc acting as an electron donor.[10–13] The orientation of the attached NDI units in **1** is drastically changed in concert with the rotation of the Cp rings of the Fc moiety (Scheme 2), and is precisely controlled by the degree of interaction between the NDI units (NDIs) during the reduction process. The columnar structure of **1** in the solid state results in n-type semiconducting behavior.

The crystal structure of **1** shows the stacked conformation (Figure 1).[14] The mean plane distance between the NDI π-planes (3.59 Å) is in agreement with that observed for intramolecular π–π interaction.[10,12] The distance is also

[*] Dr. A. Takai, Prof. Dr. M. Takeuchi
Organic Materials Group
National Institute for Materials Science (NIMS)
1-2-1 Sengen, Tsukuba, Ibaraki 305-0047 (Japan)
E-mail: TAKEUCHI.Masayuki@nims.go.jp
Homepage: http://www.nims.go.jp/macromol/english/
Dr. T. Yasuda
Organic Thin-Film Solar Cells Group
National Institute for Materials Science (NIMS)
1-2-1 Sengen, Tsukuba, Ibaraki 305-0047 (Japan)
Dr. T. Ishizuka, Prof. Dr. T. Kojima
Department of Chemistry, Graduate School of Pure and Applied Sciences, University of Tsukuba
1-1-1 Tennoudai, Tsukuba, Ibaraki 305-8571 (Japan)

[**] We are grateful to Prof. Dr. H. Oshio and Dr. J. Kuwabara for their helpful discussion. We also appreciate Dr. Y. Kobayashi for her support of UV/Vis/NIR spectroscopy in solid states. This research was supported by Grants-in-Aid for Scientific Research for Priority Area "Coordination Programming" (area 2107) to M.T., "Nanotechnology Platform Project", and Center of Materials Research for Low Carbon Emission from MEXT (Japan). A.T. appreciates support from a JSPS fellowship for young scientists.

Supporting information for this article is available on the WWW under http://dx.doi.org/10.1002/anie.201302587.

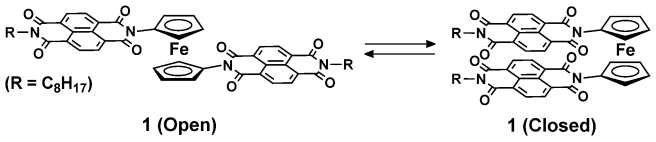

Scheme 2. The open form (left) and the closed form (right) of **1**, with a small rotational barrier.

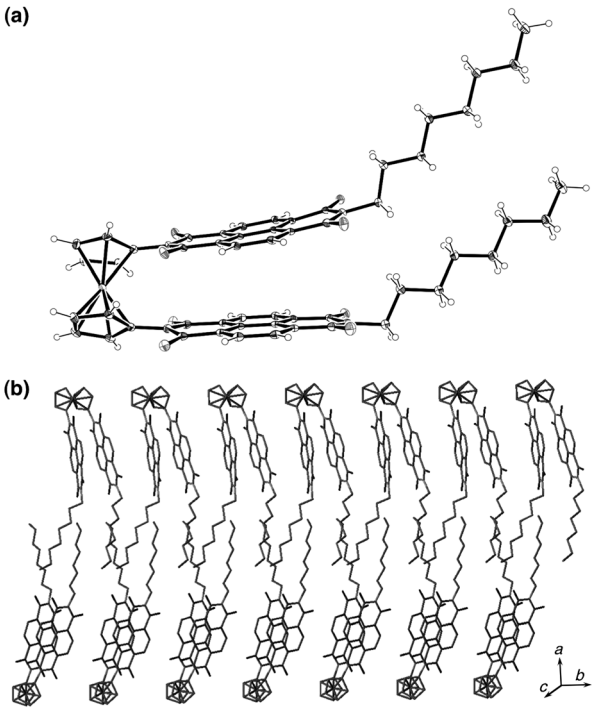

Figure 1. Crystal structure of **1**. a) An ORTEP drawing of the molecule (ellipsoids set at 50% probability). b) A view of the crystal packing. Hydrogen atoms are omitted for clarity.

comparable to that between the Cp rings of Fc (3.30 Å). It should be noted that **1** stacks in the direction of the crystallographic *b* axis through not only intermolecular π–π interactions among the NDIs but also van der Waals interactions among the octyl groups. As a result, each donor (Fc) and acceptor (NDI) unit is aligned in a columnar fashion in such a way that a net dipole moment is canceled. The calculated energy difference between the open form and the closed form (see Scheme 2) is small (1.4 kcal mol^{-1}) in the neutral state.

Variable-temperature ^{1}H NMR spectra of **1** and **2** are shown in the Supporting Information, Figures S5 and S6. The signals of the NDI protons in **1** ($\delta = 8.31$ and 8.34 ppm at 298 K) broaden with decreasing temperature, whereas those of **2** (8.78 and 8.81 ppm at 298 K) remain sharp even at 223 K.[15] These results indicate rapid interconversion of the different conformations of **1** on the ^{1}H NMR timescale at 298 K, and decrease in the rotation rate of the NDIs with decreasing temperature owing to the intramolecular interaction between the NDI units in **1**.

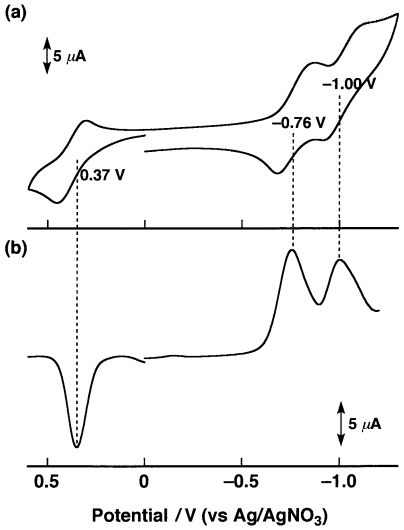

Figure 2. a) CV (100 mV s^{-1}) and b) DPV of **1** (4×10^{-4} M) in deaerated CH_2Cl_2 containing 0.1 M $TBAPF_6$.

The two NDI moieties of **1** do not show remarkable intramolecular π–π interactions at 298 K (for UV/Vis/NIR spectra, see the Supporting Information, Figures S7 and S8). However, the stacking/destacking structures of the NDI pendants can be switched in response to redox stimuli in solution. Figure 2 shows cyclic voltammogram (CV) and differential pulse voltammogram (DPV) of **1**. The CVs of Fc and **2** are also shown in the Supporting Information, Figure S9, for comparison. All of the compounds (**1**, **2**, and Fc) exhibited a one-electron oxidation process, assigned to the oxidation of the Fc moiety (Fe^{2+}/Fe^{3+}). The oxidation potential of **1** (0.37 V) is positively shifted as compared to that of **2** (0.31 V) and Fc (0.26 V), owing to the electron-withdrawing character of the NDI moieties. On the other hand, the reduction process of **1** is split into two discrete one-electron steps.[16] The first reduction potential of **1** (−0.76 V) is higher than that of **2** (−0.86 V) as a result of electronic interaction between the proximate NDIs. The second reduction of **1** occurs at a lower potential (−1.00 V) owing to the electrostatic repulsion between the NDI radical anions.

The UV/Vis/NIR spectral titration of **1** was examined by using a one-electron reductant, namely tetrakis(dimethylamino)ethylene (TDAE).[17] In CH_2Cl_2, **1** is reduced by one electron in the presence of TDAE to form $[\mathbf{1}]^{\bullet-}$ [Equation (1)], and a remarkable spectral change was observed

$$\mathbf{1} + \mathrm{TDAE} \rightarrow [\mathbf{1}]^{\bullet-} + \mathrm{TDAE}^{\bullet+} \quad (1)$$

(Figure 3 a). The UV/Vis/NIR spectrum of $[\mathbf{1}]^{\bullet-}$ is different from that of $[\mathbf{2}]^{\bullet-}$, which shows a typical spectrum assigned to a monomeric $NDI^{\bullet-}$.[18] A broad NIR absorption band at 2500 nm appeared for $[\mathbf{1}]^{\bullet-}$. No such NIR band was observed for $[\mathbf{2}]^{\bullet-}$ (Supporting Information, Figure S11), ruling out the possibility of intermolecular π-stacking between the NDIs in **1** in solution. The NIR absorption band, a so-called charge-resonance band, is ascribed to the result of negative-charge delocalization of $[\mathbf{1}]^{\bullet-}$ over the two NDIs,[10c,19] indicating that

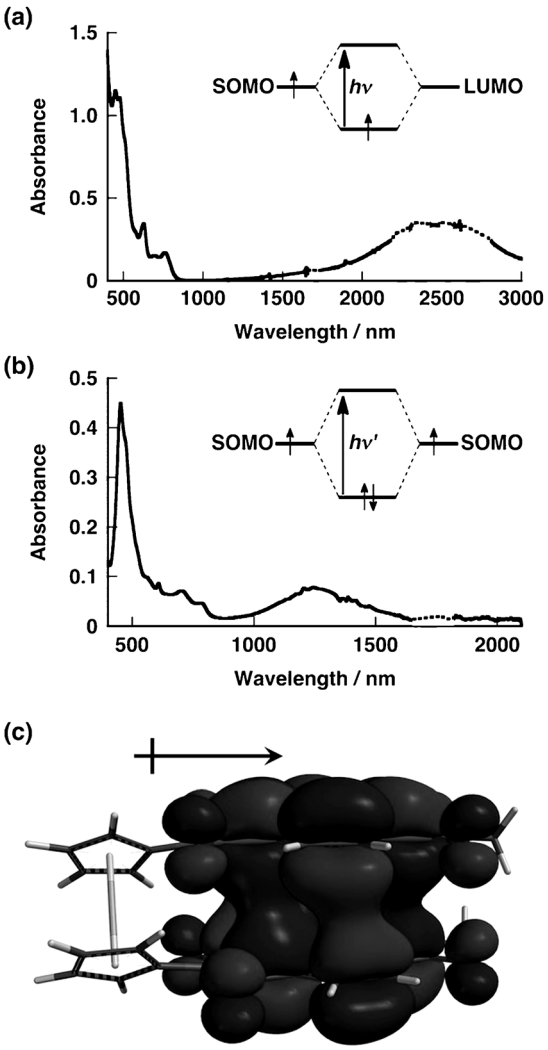

Figure 3. UV/Vis/NIR spectra of **1** in the presence of TDAE in deaerated a) CH_2Cl_2 (6.1×10^{-5} M) and b) DMF (7.3×10^{-6} M) at 298 K. In (a) and (b), the insets show molecular orbital diagrams for $[\mathbf{1}]^{\bullet-}$ and $[\mathbf{1}]^{2-}$, respectively. The absorption of the solvent is not shown and is interpolated by dotted lines. c) The SOMO of $[\mathbf{1}]^{\bullet-}$ calculated by DFT at the UB3LYP/6-31G* level. The octyl groups are replaced by methyl groups for simplicity. The arrow indicates the direction of the dipole moment (4.12 debye).

1 is in the closed form where the two NDIs are cofacially stacked as found in the crystal structure of **1**. In DMF, $[\mathbf{1}]^{\bullet-}$ can be further reduced in the presence of excess TDAE to form $[\mathbf{1}]^{2-}$ [Equation (2)].[20,21] A new NIR absorption band at 1250 nm was observed for $[\mathbf{1}]^{2-}$ (Figure 3b).

$$[\mathbf{1}]^{\bullet-} + \mathrm{TDAE} \rightarrow [\mathbf{1}]^{2-} + \mathrm{TDAE}^{\bullet+} \quad (2)$$

Spectroelectrochemical measurements allowed us to observe UV/Vis/NIR spectra that correspond to $[\mathbf{1}]^{\bullet-}$ and $[\mathbf{1}]^{2-}$ by applying potentials at −0.90 V and −1.25 V, respectively (Supporting Information, Figure S12). Those spectra are consistent with those obtained by using a chemical reductant (TDAE) as shown in Figure 3.

The SOMO of $[\mathbf{1}]^{\bullet-}$ in the optimized structure is shown in Figure 3c. In sharp contrast to the LUMO (antibonding orbital) of the neutral **1** (Supporting Information, Figure S13), the SOMO of $[\mathbf{1}]^{\bullet-}$ represents the delocalization of the negative charge and the bonding character between the two NDI π* orbitals. The charge-resonance bands observed for $[\mathbf{1}]^{\bullet-}$ and $[\mathbf{1}]^{2-}$ in the NIR region are explained as the absorptions corresponding to the electronic transitions (*hν* and *hν′*) from the bonding to the antibonding π-orbital (insets of Figure 3a and b, respectively).

The electron paramagnetic resonance (EPR) spectrum observed for a mixture of **2** and TDAE in DMF at 298 K (Figure 4a) is well-reproduced by a simulated spectrum with the hyperfine coupling constants (*hfc*) of $[\mathbf{2}]^{\bullet-}$ (1 equiv) and $TDAE^{\bullet+}$ (1 equiv), which are consistent with the reported values for the monomeric $NDI^{\bullet-}$ and $TDAE^{\bullet+}$.[11a,19a,21,22] On the other hand, the EPR spectrum obtained as a result of electron transfer from TDAE to **1** [Equation (1)] is different from that in the case of **2**. The EPR spectrum of $[\mathbf{1}]^{\bullet-}$ can be simulated with the half *hfc* values and double numbers of atoms in $[\mathbf{2}]^{\bullet-}$ (Figure 4b). Thus, the EPR spectrum of $[\mathbf{1}]^{\bullet-}$, together with the observation of the NIR absorption, indicates the spin delocalization over the two NDIs owing to the charge-resonance effect.

The EPR intensity of $[\mathbf{1}]^{2-}$ in DMF at 298 K was significantly decreased as compared to that of $[\mathbf{1}]^{\bullet-}$ (Supporting Information, Figure S15). The EPR spectrum of $[\mathbf{1}]^{2-}$ with $TDAE^{\bullet+}$ [Equation (2)] can be faithfully reproduced by a simulated spectrum with *hfc* of the monomeric $NDI^{\bullet-}$ moiety (2 equiv) and $TDAE^{\bullet+}$ (9.4 equiv), as shown in Figure 4c. Based on this ratio of the EPR intensities between $NDI^{\bullet-}$ and $TDAE^{\bullet+}$, it is determined that 21% of $[\mathbf{1}]^{2-}$ exists as a paramagnetic form and the other (79%) as a diamagnetic form at 298 K. No triplet signal for $[\mathbf{1}]^{2-}$ was observed at 108 K owing to the formation of a closed shell between the NDI radical anions (inset of Figure 3b).

With decreasing the temperature, only the EPR signal owing to $[\mathbf{1}]^{2-}$ almost disappeared (Figure 4d). This spectral change is reversible, clearly indicating the equilibrium between the paramagnetic open form and the diamagnetic closed form of $[\mathbf{1}]^{2-}$. The formation constant K of the closed form in Equation (3) is determined to be $K = 3.7 \pm 0.2$ at

$$[\mathrm{Open}] \overset{K}{\rightleftarrows} [\mathrm{Closed}] \quad (3)$$

298 K. The K values were similarly determined at various temperatures to show a linear correlation between $\ln(K)$ and T^{-1} (Figure 4e; Supporting Information, Table S2), affording a van't Hoff plot to determine thermodynamic parameters for the conformational change of $[\mathbf{1}]^{2-}$ from the open form to the closed form: $\Delta H = -5.0 \pm 0.6$ kcal mol^{-1} and $\Delta S = -13.9 \pm 2.3$ cal K^{-1} mol^{-1}.

Based on the above results, the conformational change of **1** by redox stimuli can be summarized as shown in Scheme 3. In the neutral state, the NDIs of **1** rotate fast on the NMR timescale at 298 K. This pivoting motion is modulated by temperature and electron-transfer reduction of **1**. In the one-electron reduced state, $[\mathbf{1}]^{\bullet-}$ is tightly closed because of the π-bonding interaction between the two NDIs. The stabilization

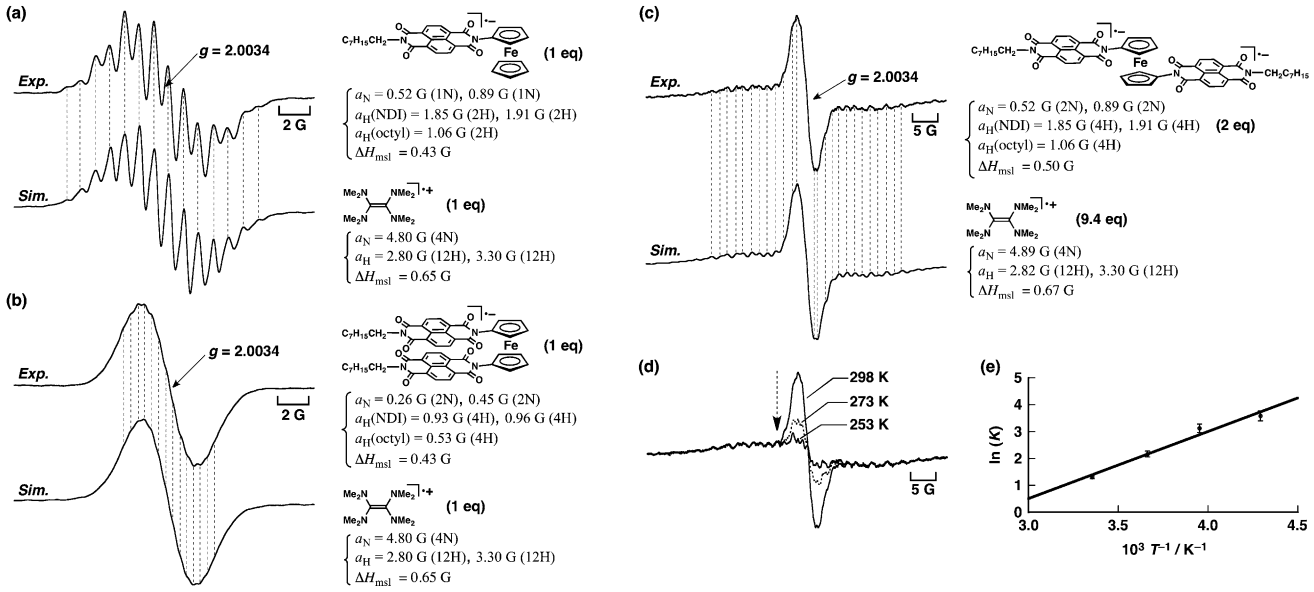

Figure 4. EPR spectra of a) $[\mathbf{2}]^{\bullet-}$ (3.4×10^{-5} M), b) $[\mathbf{1}]^{\bullet-}$ (1.7×10^{-5} M), and c) $[\mathbf{1}]^{2-}$ (1.7×10^{-5} M) generated by TDAE in deaerated DMF at 298 K,[20] and the computer-simulated spectrum with the *hfc* values and the maximum slope line widths (ΔH_{msl}). d) Temperature-dependent EPR spectral changes of $[\mathbf{1}]^{2-}$ in deaerated DMF. e) A van't Hoff plot for the formation constant of the closed form of $[\mathbf{1}]^{2-}$. Detailed EPR data for $[\mathbf{1}]^{\bullet-}$ and $[\mathbf{1}]^{2-}$ are shown in the Supporting Information, Figure S16.

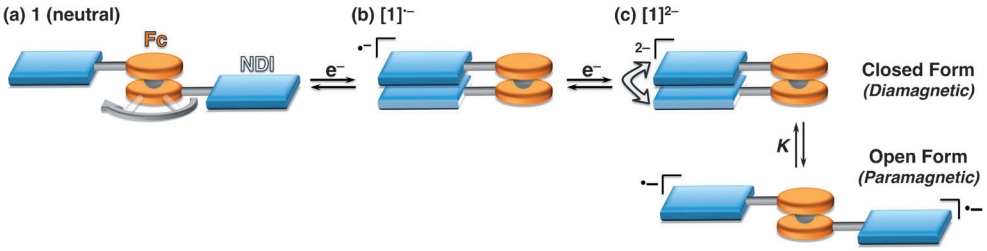

Scheme 3. Description of redox-controlled pivoting motions of **1**.

energy of this π-bonding is estimated to be 5.7 kcal mol^{-1} from the spectroscopic measurements (half the energy of λ_{max}), which is much larger than the rotational barrier of Cp rings of Fc (ca. 1 kcal mol^{-1}).[5] The closed structure of $[\mathbf{1}]^{\bullet-}$ is unclenched by further reduction owing to the balance of the electronic interaction and the electrostatic repulsion between the NDI radical anions; thereby, $[\mathbf{1}]^{2-}$ exhibits the equilibrium between the closed form (diamagnetic) and the open form (paramagnetic).

As a preliminary application of **1** to construction of functional materials, an organic field-effect transistor (OFET) was prepared using the compound. In the solid state, the NDI moieties in **1** stack together not only by intramolecular but also by intermolecular π–π interactions. Such a conduit composed of the redox-active π-conjugated molecules can be applied to electronic devices; the thin film (57 nm) of **1** fabricated using vacuum vapor method exhibited the OFET performance (Supporting Information, Figures S17 and S18).

In summary, we have demonstrated that π–π interactions between two π-conjugated systems can be regulated by redox reactions of the aromatic moieties that are directly linked to a molecular rotator. In **1**, the orientations of the NDI pendants attached to the Fc moiety are confined by the two-dimensional pivoting motion of the Fc rotator. The stacking behaviors are elucidated quantitatively in each electron-transfer state on the basis of spectroscopic measurements: the open and the closed forms are clearly controlled by the electronic interactions of NDI moieties during the reduction process. The direct linkage between the NDI moieties and the molecular rotator (Fc) is essential to precisely control the dynamic orientation of the NDI moieties. Such a promising new approach can be generalized for a variety of NDI-Fc-NDI derivatives. Further developments of molecular devices based on the NDI-Fc-NDI framework are in progress in our laboratory to foster organic actuators and stimuli-responsive molecular switches for new functional materials.

Received: March 28, 2013
Revised: June 2, 2013
Published online: July 23, 2013

Keywords: donor–acceptor systems · electronic structure · materials science · π interactions · stacking interactions

[1] a) B. L. Feringa, *Molecular Switches*, Wiley-VCH, Weinheim, **2001**; b) V. Balzani, M. Venturi, A. Credi, *Molecular Devices and Machines*, Wiley-VCH, Weinheim, **2003**; c) P. A. Anquetil, J. D. Madden, H.-h. Yu, T. M. Swager, I. W. Hunter in *Handbook of Organic Electronics and Photonics*, *Vol. 1* (Ed.: H. S. Nalwa), American Scientific Publishers, Los Angeles, **2007**, pp. 447; d) C.

Song, T. M. Swager, *Org. Lett.* **2008**, *10*, 3575; e) A. C. Fahrenbach, Z. X. Zhu, D. Cao, W.-G. Liu, H. Li, S. K. Dey, S. Basu, A. Trabolsi, Y. Y. Botros, W. A. Goddard, J. F. Stoddart, *J. Am. Chem. Soc.* **2012**, *134*, 16275; f) V. Dehm, M. Büchner, J. Seibt, V. Engel, F. Würthner, *Chem. Sci.* **2011**, *2*, 2094; g) E. Ohta, H. Sato, S. Ando, A. Kosaka, T. Fukushima, D. Hashizume, M. Yamasaki, K. Hasegawa, A. Muraoka, H. Ushiyama, K. Yamashita, T. Aida, *Nat. Chem.* **2011**, *3*, 68; h) A. Iordache, M. Retegan, F. Thomas, G. Royal, E. Saint-Aman, C. Bucher, *Chem. Eur. J.* **2012**, *18*, 7648; i) D. Bléger, T. Liebig, R. Thiermann, M. Maskos, J. P. Rabe, S. Hecht, *Angew. Chem.* **2011**, *123*, 12767; *Angew. Chem. Int. Ed.* **2011**, *50*, 12559.

[2] a) T. Sakai, T. Satou, T. Kaikawa, K. Takimiya, T. Otsubo, Y. Aso, *J. Am. Chem. Soc.* **2005**, *127*, 8082; b) H. Yoo, J. Yang, A. Yousef, M. R. Wasielewski, D. Kim, *J. Am. Chem. Soc.* **2010**, *132*, 3939; c) S. Mukhopadhyay, S. P. Jagtap, V. Coropceanu, J. L. Brédas, D. M. Collard, *Angew. Chem.* **2012**, *124*, 11797; *Angew. Chem. Int. Ed.* **2012**, *51*, 11629; d) F. Schlosser, M. Moos, C. Lambert, F. Würthner, *Adv. Mater.* **2013**, *25*, 410.

[3] a) G. S. Kottas, L. I. Clarke, D. Horinek, J. Michl, *Chem. Rev.* **2005**, *105*, 1281; b) E. R. Kay, D. A. Leigh, F. Zerbetto, *Angew. Chem.* **2007**, *119*, 72; *Angew. Chem. Int. Ed.* **2007**, *46*, 72; c) J. B. Wang, A. Kulago, W. R. Browne, B. L. Feringa, *J. Am. Chem. Soc.* **2010**, *132*, 4191; d) T. Kudernac, N. Ruangsupapichat, M. Parschau, B. Macia, N. Katsonis, S. R. Harutyunyan, K. H. Ernst, B. L. Feringa, *Nature* **2011**, *479*, 208; e) M. Shibata, S. Tanaka, T. Ikeda, S. Shinkai, K. Kaneko, S. Ogi, M. Takeuchi, *Angew. Chem.* **2013**, *125*, 415; *Angew. Chem. Int. Ed.* **2013**, *52*, 397.

[4] T. Muraoka, K. Kinbara, T. Aida, *Nature* **2006**, *440*, 512.

[5] a) X. B. Wang, B. Dai, H. K. Woo, L. S. Wang, *Angew. Chem.* **2005**, *117*, 6176; *Angew. Chem. Int. Ed.* **2005**, *44*, 6022; b) J. D. Crowley, I. M. Steele, B. Bosnich, *Chem. Eur. J.* **2006**, *12*, 8935; c) B. D. Koivisto, A. S. Ichimura, R. McDonald, M. T. Lemaire, L. K. Thompson, R. G. Hicks, *J. Am. Chem. Soc.* **2006**, *128*, 690.

[6] a) T. Ikeda, S. Shinkai, K. Sada, M. Takeuchi, *Tetrahedron Lett.* **2009**, *50*, 2006; b) J. Yoshino, E. Hasegawa, N. Hayashi, H. Higuchi, *Tetrahedron Lett.* **2011**, *52*, 4295; c) A. Iordache, M. Oltean, A. Milet, F. Thomas, B. Baptiste, E. Saint-Aman, C. Bucher, *J. Am. Chem. Soc.* **2012**, *134*, 2653.

[7] N. M. Shavaleev, E. S. Davies, H. Adams, J. Best, J. A. Weinstein, *Inorg. Chem.* **2008**, *47*, 1532.

[8] A. Shafir, M. P. Power, G. D. Whitener, J. Arnold, *Organometallics* **2000**, *19*, 3978.

[9] a) C. J. McAdam, B. H. Robinson, J. Simpson, *Organometallics* **2000**, *19*, 3644; b) M. Sato, S. Ebine, S. Akabori, *Synthesis* **1981**, 472.

[10] a) R. S. Lokey, B. L. Iverson, *Nature* **1995**, *375*, 303; b) J. J. Reczek, K. R. Villazor, V. Lynch, T. M. Swager, B. L. Iverson, *J. Am. Chem. Soc.* **2006**, *128*, 7995; c) N. Ashkenasy, W. S. Horne, M. R. Ghadiri, *Small* **2006**, *2*, 99; d) Y. S. Chong, W. R. Carroll, W. G. Burns, M. D. Smith, K. D. Shimizu, *Chem. Eur. J.* **2009**, *15*, 9117.

[11] a) S. V. Bhosale, C. H. Jani, S. J. Langford, *Chem. Soc. Rev.* **2008**, *37*, 331; b) M. Supur, M. E. El-Khouly, J. H. Seok, K. Y. Kay, S. Fukuzumi, *J. Phys. Chem. A* **2011**, *115*, 14430.

[12] a) B. A. Jones, A. Facchetti, T. J. Marks, M. R. Wasielewski, *Chem. Mater.* **2007**, *19*, 2703; b) H. Yan, Z. Chen, Y. Zheng, C. Newman, J. R. Quinn, F. Dotz, M. Kastler, A. Facchetti, *Nature* **2009**, *457*, 679; c) X. Zhan, A. Facchetti, S. Barlow, T. J. Marks, M. A. Ratner, M. R. Wasielewski, S. R. Marder, *Adv. Mater.* **2011**, *23*, 268.

[13] a) N. Sakai, J. Mareda, E. Vauthey, S. Matile, *Chem. Commun.* **2010**, *46*, 4225; b) N. Sakai, R. Bhosale, D. Emery, J. Mareda, S. Matile, *J. Am. Chem. Soc.* **2010**, *132*, 6923; c) F. Würthner, M. Stolte, *Chem. Commun.* **2011**, *47*, 5109; d) C. Wang, H. Dong, W. Hu, Y. Liu, D. Zhu, *Chem. Rev.* **2012**, *112*, 2208.

[14] Crystallographic data for **1** are given in the Supporting Information, Table S1. CCDC 921589 contains the supplementary crystallographic data for this paper. These data can be obtained free of charge from The Cambridge Crystallographic Data Centre via www.ccdc.cam.ac.uk/data_request/cif.

[15] The NDI protons of **1** shifted upfield as compared to those of **2** and **3** ($\delta = 8.75$ ppm), which may result from the ring-current effect of the other NDI moiety in the closed conformation of **1**. Similar chemical shift changes were observed for both **1** and **2** at different temperatures.

[16] Each current intensity at -0.76 V and -1.00 V of **1** is nearly the same as that of the one-electron oxidation process that is due to the Fc moiety. This result clearly indicates that the first two-electron reduction processes of **1** are both one-electron processes. The dianion of **3** ($[\mathbf{3}]^{2-}$) was formed at -1.35 V, whereas the third and fourth reduction processes were not observed for **1**, which is probably because of the large electrostatic repulsion between the doubly charged NDIs in **1**.

[17] The UV/Vis/NIR spectral change of **1** on addition of a one-electron oxidant in CH_2Cl_2 is shown in the Supporting Information, Figure S10.

[18] a) D. Gosztola, M. P. Niemczyk, W. Svec, A. S. Lukas, M. R. Wasielewski, *J. Phys. Chem. A* **2000**, *104*, 6545; b) S. Guha, F. S. Goodson, L. J. Corson, S. Saha, *J. Am. Chem. Soc.* **2012**, *134*, 13679.

[19] a) J.-F. Penneau, B. J. Stallman, P. H. Kasai, L. L. Miller, *Chem. Mater.* **1991**, *3*, 791; b) L. L. Miller, K. R. Mann, *Acc. Chem. Res.* **1996**, *29*, 417; c) V. Ganesan, S. V. Rosokha, J. K. Kochi, *J. Am. Chem. Soc.* **2003**, *125*, 2559; d) J. J. Novoa, P. W. Stephens, M. Weerasekare, W. W. Shum, J. S. Miller, *J. Am. Chem. Soc.* **2009**, *131*, 9070.

[20] The oxidation potential of TDAE is comparable with the first reduction potential of **1**, and it was difficult to form $[\mathbf{1}]^{2-}$ in CH_2Cl_2 (see Ref. [21]). Thus, more polar solvents such as DMF is appropriate for the formation of $[\mathbf{1}]^{2-}$, because the oxidation potential of TDAE in DMF is lower than that in CH_2Cl_2 and the reduction potential of **1** in DMF is higher than that in CH_2Cl_2. To form $[\mathbf{1}]^{\bullet-}$ and $[\mathbf{1}]^{2-}$, 8 equiv and 20 equiv of TDAE were added to a DMF solution of **1**, respectively.

[21] a) J. M. Fritsch, H. Weingarten, J. D. Wilson, *J. Am. Chem. Soc.* **1970**, *92*, 4038; b) K. Kuwata, D. H. Geske, *J. Am. Chem. Soc.* **1964**, *86*, 2101.

[22] Similar EPR spectra were observed for the one-electron reduced species of **1** and **2** in the presence of TDAE in CH_2Cl_2 at 298 K (Supporting Information, Figure S14), corresponding to the UV/Vis/NIR spectroscopic results.

